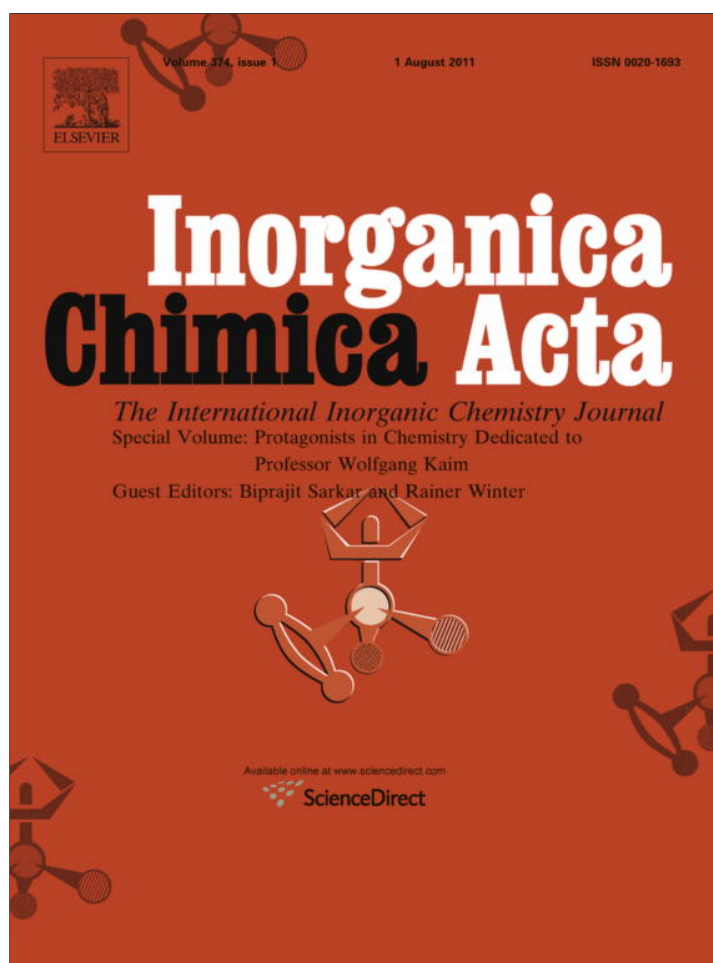


Provided for non-commercial research and education use.
Not for reproduction, distribution or commercial use.



This article appeared in a journal published by Elsevier. The attached copy is furnished to the author for internal non-commercial research and education use, including for instruction at the authors institution and sharing with colleagues.

Other uses, including reproduction and distribution, or selling or licensing copies, or posting to personal, institutional or third party websites are prohibited.

In most cases authors are permitted to post their version of the article (e.g. in Word or Tex form) to their personal website or institutional repository. Authors requiring further information regarding Elsevier's archiving and manuscript policies are encouraged to visit:

<http://www.elsevier.com/copyright>



Contents lists available at ScienceDirect

Inorganica Chimica Acta

journal homepage: www.elsevier.com/locate/ica

Influence of the linker length on the host–guest properties of alkoxy- and polypyridine-bridged molecular rectangles of formulae $\{[\text{Re}(\text{CO})_3(\text{OC}_5\text{H}_{11})]_4(\text{L})_2\}$, with L = 4-pyridinealdazine and 4,4'-azobis(pyridine)

Faustino Eduardo Morán Vieyra^a, Mauricio Cattaneo^a, Florencia Fagalde^a, Fernando Bozoglian^b, Antoni Llobet^b, Néstor E. Katz^{a,*}

^a INQUINOA–CONICET, Instituto de Química Física, Facultad de Bioquímica, Química y Farmacia, Universidad Nacional de Tucumán, Ayacucho 471, (T4000INI) San Miguel de Tucumán, Argentina

^b Institut Català d'Investigació Química (ICIQ), Campus Universitari de Tarragona, Av. Paisos Catalans 16, E-43007 Tarragona, Spain

ARTICLE INFO

Article history:

Available online 4 March 2011

Dedicated to Prof. Wolfgang Kaim.

Keywords:

Rhenium complexes
Molecular rectangles
Host–guest interactions
Fluorescence quenching
Detection of aromatic hydrocarbons

ABSTRACT

A new series of alkoxy- and polypyridine-bridged rhenium molecular rectangles of formulae $\{[\text{Re}(\text{CO})_3(\text{OC}_5\text{H}_{11})]_4(\text{L})_2\}$, with OC_5H_{11} = 1-pentoxo, L = PCA (4-pyridinecarboxaldehyde azine) and 4,4'-azpy (4,4'-azobis(pyridine)), were synthesized and characterized by spectroscopic and diffraction techniques. Quenching of fluorescence of aromatic hydrocarbons by these complexes was studied by stationary and dynamic techniques. The quenching mechanism proved to be predominantly static and the Stern–Volmer constants indicated a decrease of the extent of C–H... π interactions with decreasing length of the linkers that form the molecular rectangles.

© 2011 Elsevier B.V. All rights reserved.

1. Introduction

Host–guest chemistry is relevant to environmental applications since it can be used for the detection of traces of certain contaminants. In addition, photophysical properties have long been recognized as very important for analytical purposes, due to their high selectivity detection level. Metal-containing molecular triangles, squares, and rectangles can act as hosts and their utilization as sensors will depend on the size of the host, the properties of the guests and the different interactions between them [1–4].

In the last decade, considerable advances have been accomplished in the synthesis and uses of tricarbonylrhenium(I) complexes with shapes of triangles [1,5], squares [5–7], rectangles [3,8,9] and heteronuclear systems [10]. In particular, rhenium(I) tricarbonyl diimine complexes can be used as corners of molecular rectangles where the spacers are alkoxy-groups. Thus, when $[\text{Re}_2(\text{CO})_{10}]$ is treated with pyridine ligands in the presence of aliphatic alcohols under refluxing conditions, alkoxy-bridged molecular rectangles can be obtained in a self-assembly way with acceptable yields [3,11]. The photophysical properties of some of these squares were studied, and the species

$\{[\text{Re}(\text{CO})_3(\text{OC}_5\text{H}_{11})]_4(4,4'\text{-bpy})_2\}$ (4,4'-bpy = 4,4'-bipyridine) can form a complex with pyrene, as reported by Lu et. al. [11]. In these systems, non-covalent CH... π interactions between soft acids (CH groups) and soft bases (π groups) were detected. Association constants showed static and dynamic effects [11].

In this work, we have synthesized the novel molecular rectangles $\{[\text{Re}(\text{CO})_3(\text{OC}_5\text{H}_{11})]_4(\text{PCA})_2\}$ (isomers **1** and **2**), and $\{[\text{Re}(\text{CO})_3(\text{OC}_5\text{H}_{11})]_4(4,4'\text{-azpy})_2\}$ **3**, with OC_5H_{11} = 1-pentoxo, PCA = 4-pyridinecarboxaldehyde azine (or 4-pyridinaldazine or 1,4-bis(4-pyridyl)-2,3-diaza-1,3-butadiene) and 4,4'-azpy = 4,4'-azobis(pyridine). The last two bridging ligands have two nitrogens in the middle of the bridge; these extra lone pair of electrons could change the environmental selectivity and the electronic interactions with the guests. It can be predicted that the compounds described in this work will be useful as sensors of powerful environmental contaminants such as polycyclic aromatic hydrocarbons.

2. Materials and methods

2.1. Physical measurements

Reagents were analytical reagent grade and were used as received without further purification. UV–vis absorption spectra were recorded on a Varian Cary 50 spectrophotometer, using

* Corresponding author.

E-mail address: nkatz@fbqf.unt.edu.ar (N.E. Katz).

1-cm quartz cells. Infrared spectra were obtained as KBr pellets, with a Perkin–Elmer Spectrum RX-1 FTIR spectrometer. Luminescence spectra were measured with a Shimadzu RF-5301 PC spectrofluorometer, provided with 1-cm fluorescence cells. Luminescence decay times were determined by using a homemade pulse luminescence system composed by a PTI 101 Monochromator ($f/4$, 1200 blazes), with a Hamamatsu R928 PMT attached to the output slit. The signals were fed to a digital oscilloscope (Tektronix TSB3032, 300 MHz) and analyzed with Origin[®] Microcal 7.0 software. An excitation source at $\lambda = 355$ nm (10 ns FWHM, 5 mJ/pulse), output of a Nd:Yag laser (Minilite II, Continuum, USA), was used. Chemical analyses for C, H, N and S were carried out at INQUIMAE, University of Buenos Aires, Argentina, with an estimated error of $\pm 0.5\%$. NMR spectra were recorded on a Bruker Advance 500 spectrometer (500 MHz for ^1H and 125 MHz for ^{13}C). Mass Spectra (ESI) were recorded on a Waters LCT Premier spectrometer.

2.2. X-ray structure determination

Crystals of complex **1** were obtained by slow diffusion of Et_2O into a CD_2Cl_2 solution. Measurements were made on a Bruker-Nonius diffractometer equipped with a APPEX2 4 K CCD area detector, a FR591 rotating anode with Mo $K\alpha$ radiation, Montel mirrors as monochromator and a Kryoflex low temperature device ($T = -173$ °C). Full-sphere data collection was used with ω and ϕ scans. Programs used: Data collection Apex2 V. 1.0-22 (Bruker-Nonius 2004), data reduction SAINT+Version 6.22 (Bruker-Nonius 2001) and absorption correction SADABS V. 2.10 (2003). For structure solution and refinement, the SHELXTL Version 6.14 (Sheldrick, 2008) program was used [12].

2.3. Fluorescence quenching studies

Quenching of fluorescence of anthracene and pyrene by the synthesized molecular rectangles was carried out under aerated conditions. The excitation wavelengths were $\lambda_{\text{exc}} = 336$ nm (for pyrene) and $\lambda_{\text{exc}} = 340$ nm (for anthracene), using THF as solvent. The monitoring wavelengths were chosen as the emission maxima: $\lambda_{\text{em}} = 373$ nm (for pyrene) and $\lambda_{\text{em}} = 401$ nm (for anthracene). Relative fluorescence intensities were measured for solutions at different quencher concentrations. No changes in shape of the emission spectra were detected, but the fluorescence intensities did follow a Stern–Volmer (SV) relationship, $I_0/I = 1 + K_{\text{SV}} [Q]$, where I_0 and I were the emission intensities in the absence and presence of quencher, respectively, and $[Q]$ was the quencher concentration. The quenching rates were obtained from the Stern–Volmer constants, K_{SV} . Excited-state lifetime studies of pyrene were determined by analyzing the decays as a sum of exponential functions, thus allowing the partial elimination of instrument time broadening and rendering a temporal resolution. A triangular cell in front-face mode was used in stationary fluorescence quenching experiments in order to minimize inner filter effects [13].

3. Experimental

3.1. Synthesis of $\{[\text{Re}(\text{CO})_3(\mu\text{-OC}_5\text{H}_{11})]_4(\mu\text{-PCA})_2\}$, (**1**) and (**2**)

Synthetic procedures can include a two-step process [6] or a one-step process [9,14]. In this work, we have followed Mandáls synthetic method [14]. A mixture of 200 mg (0.31 mmol) of $[\text{Re}_2(\text{CO})_{10}]$ and 65 mg (0.31 mmol) of PCA in 10 mL of 1-pentanol was heated under reflux and stirred for 8 h in a 50 mL flask. During that time, the pale yellow solution changed to an intense orange cloudy solution which was cooled at room temperature. Then,

10 mL of hexane were added to favor precipitation. The solid was filtered (137 mg) and then suspended in CH_2Cl_2 and filtered. Two fractions of complexes were obtained: (**1**) soluble in CH_2Cl_2 (20 mg), and (**2**) insoluble in CH_2Cl_2 (107 mg). Only crystals of (**1**) could be obtained, as described in Section 2.2. For (**1**): Yield, 4%. Chem. Anal. Found: C, 36.7; H, 3.6; N, 6.1. Calc. for $\text{C}_{56}\text{H}_{64}\text{N}_8\text{O}_{16}\text{Re}_4$: C, 36.4; H, 3.5; N, 6.1%. IR (KBr, cm^{-1}): ν_{CO} 2021 (s), 2006 (s), 1890 (vs), 1880 (vs). ^1H NMR (500 MHz, CD_2Cl_2): δ 8.51 (s, 4H, H^{a}), 8.45 (dd, $J = 5.1$ Hz, $J' = 1.3$ Hz, 8H, H^{c}), 7.44 (dd, $J = 5.3$ Hz, $J' = 1.5$ Hz, 8H, H^{b}), 4.36 (br, 8H, H^{d}), 2.10 (m, 8H, H^{e}), 1.43 (m, 16H, $\text{H}^{\text{f,g}}$), 1.01 (t, $J = 7.3$ Hz, 12H, H^{h}). ^{13}C NMR (125 MHz, CD_2Cl_2): δ 198, (2:1 CO, $\text{C}^{\text{k,k'j}}$), 197.7 (C^{i}), 152.5 (C^{a}), 152.1 (C^{c}), 124.2 (C^{b}), 82.4 (C^{d}), 33.6 (C^{e}), 27.0 (C^{f}), 22.6 (C^{g}), 13.7 (C^{h}) ppm. UV–vis (in THF): λ_{max} (nm): 410, 280. ESIMS: m/z 1873.1 ($\text{M}+\text{Na}$)⁺. For (**2**): Yield 58%. Chem. Anal. Found: C, 37.0; H, 3.6; N, 6.3. Calc. for $\text{C}_{56}\text{H}_{64}\text{N}_8\text{O}_{16}\text{Re}_4$: C, 36.4; H, 3.5; N, 6.1%. IR (KBr, cm^{-1}): ν_{CO} 2021 (s), 2006 (s), 1890 (vs), 1880 (vs). ^1H NMR (500 MHz, $(\text{CD}_3)_2\text{CO}$): δ 8.71 (s, 4H, H^{a}), 8.60 (d, $J = 6.6$ Hz, 8H, H^{c}), 7.73 (d, $J = 6.6$ Hz, 8H, H^{b}), 4.39 (br, 8H, H^{d}), 2.16 (m, 8H, H^{e}), 1.46 (m, 16H, $\text{H}^{\text{f,g}}$), 0.99 (t, $J = 7.0$ Hz, 12H, H^{h}). ^{13}C NMR (125 MHz, CD_2Cl_2): δ 152.4 (C^{a}), 124.0 (C^{b}), 81.7 (C^{d}), 32.9 (C^{e}), 27.1 (C^{f}), 22.3 (C^{g}), 13.4 (C^{h}) ppm. UV–vis (in THF): λ_{max} (nm): 410, 280. ESIMS: m/z 1873.1 ($\text{M}+\text{Na}$)⁺.

3.2. Synthesis of $\{[\text{Re}(\text{CO})_3(\mu\text{-OC}_5\text{H}_{11})]_4(\mu\text{-4,4'azpy})_2\}$. $\text{CH}_3\text{C}(\text{O})\text{CH}_3$ (**3**)

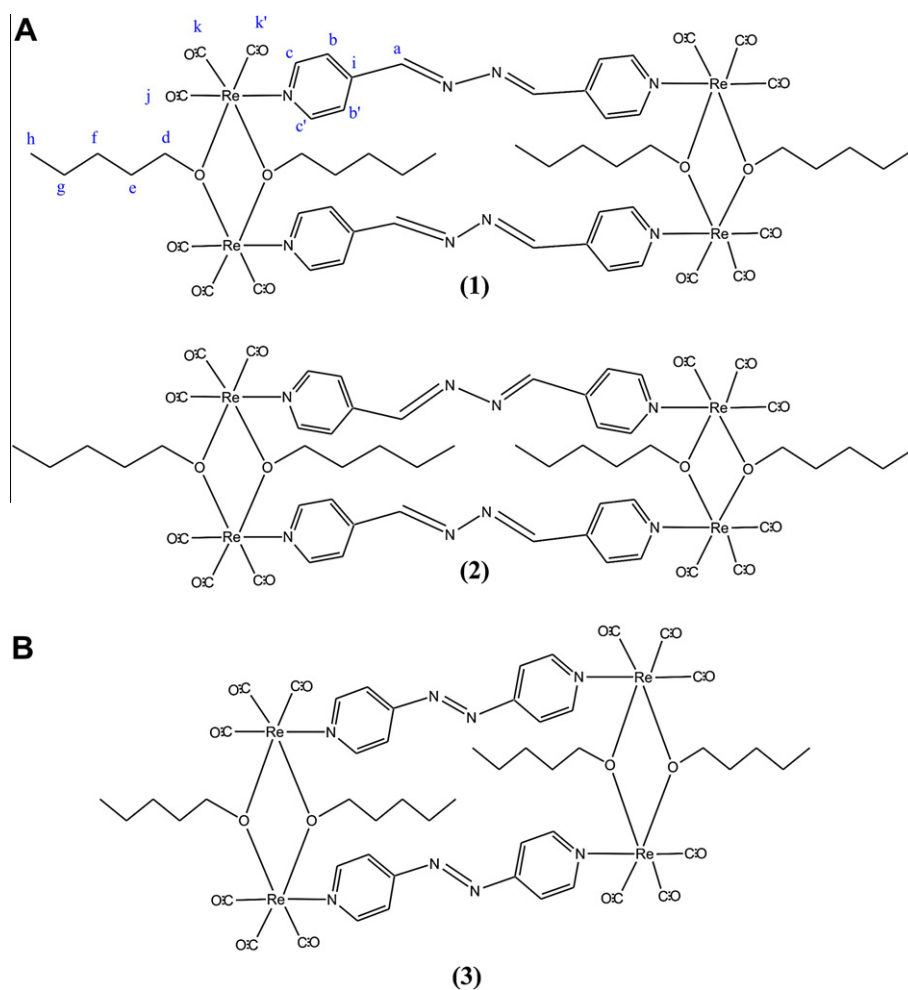
A mixture of 200 mg (0.31 mmol) of $[\text{Re}_2(\text{CO})_{10}]$ and 60 mg (0.31 mmol) of 4,4'-azpy in 10 mL of 1-pentanol was heated under reflux with continuous stirring for 8 h in a 50-mL flask. The orange solution changed to an intense red solution which was cooled at room temperature and then left for 48 h in a freezer. The red precipitate was filtered, redissolved in acetone (2 mL) and precipitated with hexane (10 mL). Yield: 160 mg (30%). Chem. Anal. Found: C, 35.6; H, 3.4; N, 6.6. Calc. for $\text{C}_{55}\text{H}_{66}\text{N}_8\text{O}_{17}\text{Re}_4$: C, 35.6; H, 3.6; N, 6.0%. IR (KBr, cm^{-1}): ν_{CO} 2021, 2006, 1885 cm^{-1} . ^1H NMR (500 MHz, CD_2Cl_2): δ 8.61 (d, $J = 8$ Hz, 8H, H^{c}), 7.51 (d, $J = 8.5$ Hz, 8H, H^{b}), 4.40 (t, $J = 10$ Hz, 8H, H^{d}), 2.13 (m, $J = 8$ Hz, 8H, H^{e}), 1.51–1.48 (m, $J = 8$ Hz, 16H, $\text{H}^{\text{f,g}}$), 1.03 (t, $J = 8.5$ Hz, 12H, H^{h}). ESIMS: m/z 1821.4 ($\text{M}+\text{Na}$)⁺.

4. Results and discussion

4.1. Syntheses and characterization

The new alkoxy-bridged rectangles complexes **1**, **2** and **3** have been obtained in solvothermal conditions with the desired ligand (PCA or 4,4'-azpy) in 1-pentanol. For PCA as a bridging ligand, two isomers have been obtained: their chemical analysis, UV–vis spectra, IR spectra were the same but there were slight differences in their NMR spectra and mass spectrometric data. The solubilities in CH_3CN and CH_2Cl_2 were different for both. For 4,4'-azpy as a bridging ligand, only one isomer has been obtained and it was soluble in CH_3CN , CH_2Cl_2 and THF. Scheme 1 shows the proposed structures and NMR numbering for complexes **1–3**. Chemical analyses and all spectroscopic data are consistent with the formation of molecular rectangles of high stability.

IR spectra for complexes **1–3** exhibit 4 intense bands corresponding to carbonyl stretching frequencies ν_{CO} , with similar patterns to those of other rhenium molecular rectangles [10]. This result is consistent with D_{2h} symmetry. Fig. 1 shows the UV–vis spectra for complexes **1** and **3** in THF at room temperature. The intense bands at $\lambda_{\text{max}} = 280$ nm ($\epsilon = 6.5 \times 10^4 \text{ M}^{-1} \text{ cm}^{-1}$) and 270 nm ($\epsilon = 4.5 \times 10^4 \text{ M}^{-1} \text{ cm}^{-1}$) for **1** and **3**, respectively, can be attributed to intraligand (IL) transitions. The broad bands at $\lambda_{\text{max}} = 410$ nm ($\epsilon = 1.3 \times 10^4 \text{ M}^{-1} \text{ cm}^{-1}$) and 450 nm ($\epsilon = 7.0 \times 10^3 \text{ M}^{-1} \text{ cm}^{-1}$) for



Scheme 1. Structure and NMR assignments for (A) $\{[\text{Re}(\text{CO})_3(\mu\text{-OC}_5\text{H}_{11})]_4(\mu\text{-PCA})_2\}$, **1** and **2**, and (B) $\{[\text{Re}(\text{CO})_3(\mu\text{-OC}_5\text{H}_{11})]_4(\mu\text{-4,4'-azpy})_2\}$, **3**.

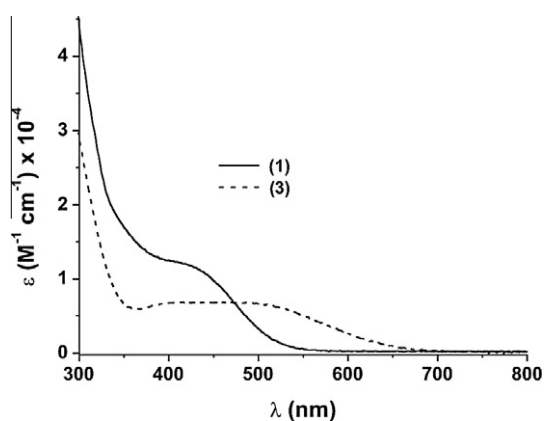


Fig. 1. UV-vis spectra for complexes $\{[\text{Re}(\text{CO})_3(\mu\text{-OC}_5\text{H}_{11})]_4(\mu\text{-PCA})_2\}$, **1** and $\{[\text{Re}(\text{CO})_3(\mu\text{-OC}_5\text{H}_{11})]_4(\mu\text{-4,4'-azpy})_2\}$, **3**, in THF at r.t.

1 and **3**, respectively, can be assigned to $d_{\pi}(\text{Re}) \rightarrow \pi^*(\text{PCA})$ and $d_{\pi}(\text{Re}) \rightarrow \pi^*(4,4'\text{-azpy})$ metal-to-ligand charge transfer (MLCT) transitions. These spectral data are similar to those of previously described molecular rectangles [9,14].

Due to the symmetry of the molecular rectangles **1** and **2**, only 3 signals were detected for the protons of PCA (see Section 3), which were slightly different according to their different conformations and slightly shifted respect to the values corresponding to the free ligand [15]. The values for chemical shifts of protons of bridging

pentanol have no differences between both species. For **3**, its ^1H NMR spectrum shows that these shifts are also unaltered, while 2 signals appear at low fields, corresponding to the protons of 4,4'-azpy. Mass spectrometry of complexes **1** and **2** showed different patterns of fragmentation, suggesting different conformations.

The crystal structure of complex **1** has been solved by X-ray diffraction analysis, confirming the rectangle architecture, with each rhenium atom coordinated to three terminal CO groups in a facial arrangement, two bridging pentyloxo ligands and one bridging PCA ligand. This structure is very similar to that of the related complex bridged by 4,4'-bpy [14]. Fig. 2 shows an ORTEP diagram of the complex, whereas its main crystallographic data are reported in Table 1, Table 2 and Supporting Information. A zig-zag structure with an eclipsed conformation is disclosed. Complex **1** shows a molecular rectangle framework with dimensions of $3.39 \times 11.57 \text{ \AA}$, as defined by Re centers with an octahedral symmetry distorted due to the Re–O–Re bridges. The structure of isomer **2** could not be determined, but probably it can be assigned to a *gauche* conformation, as shown in Scheme 1. Previous reports on related systems have demonstrated that small variations in the orientation of the ligands within the rectangular cycle can lead to the formation of crystallographic isomers [16].

4.2. Luminescence quenching studies

Complex **1** proved to be unstable in THF solution; therefore, this complex was not used for studying the luminescence quenching of

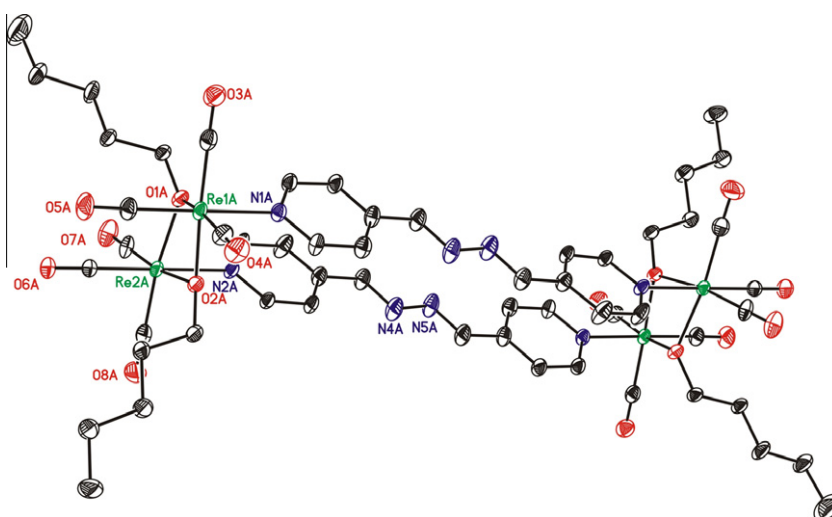


Fig. 2. ORTEP diagram of $[\text{Re}(\text{CO})_3(\mu\text{-OC}_5\text{H}_{11})]_4(\mu\text{-PCA})_2$, **1**.

Table 1
Crystal data and structure refinement for complex **1**.

Empirical formula	$\text{C}_{57} \text{H}_{70} \text{Cl}_2 \text{N}_8 \text{O}_{16} \text{Re}_4$
Formula weight	1938.91
Wavelength	0.71073 Å
Crystal system	triclinic
Space group	\bar{P}
Unit cell dimensions	$a = 10.9063(5)$ Å $b = 15.4920(8)$ Å $c = 21.3523(10)$ Å
Volume	$3383.0(3)$ Å ³
Z	2
Temperature	100(2) K
D_{calc}	1.903 mg/m ³
Absorption coefficient	7.279 mm^{-1}
Goodness-of-fit on F^2	1.030
Final R indices [$I > 2\sigma(I)$]	$R_1 = 0.0433$, $wR^2 = 0.1123$
R indices (all data)	$R_1 = 0.0642$, $wR^2 = 0.1252$

Table 2
Relevant distances and angles for complex **1**.

Relevant distances (Å) and angles (°)			
Re1A–N1A	2.210(3)	Re2A–N2A	2.210(3)
Re1A–O1A	2.125(2)	Re2A–O1A	2.133(2)
Re1A–O2A	2.135(3)	Re2A–O2A	2.128(2)
Re1A–C25A	1.903(3)	Re2A–C28A	1.915(3)
Re1A–C26A	1.904(4)	Re2A–C29A	1.890(3)
Re1A–C27A	1.922(3)	Re2A–C30A	1.912(4)
O1A–Re1A–O2A	72.40(8)	O1A–Re2A–N2A	83.60(10)

hydrocarbons. No changes were detected in the absorption spectra of complexes **2** and **3** with pyrene or anthracene, indicating a weak association in the ground state [11]. Normally, these rhenium rectangles are non-emissive, due to vibronic coupling. It is known, for example, that the $^3n - \pi^*$ excited state of 4,4'-azpy quenches the emission from the $^3\text{MLCT}$ excited state in the species $[\text{Re}(\text{bpy})(\text{CO})_3(4,4'\text{-azpy})]^+$ [17]. Although complexes **1–3** do not emit at room temperature, **2** and **3** proved to be efficient quenchers of the luminescence from anthracene and pyrene, as shown in Fig. 3 for the case of complex **2**. In this case, quenching is the result of intramolecular energy transfer from the emitting $\pi - \pi^*$ excited state of the guest to the low-lying MLCT charge transfer excited state of the host which returns to the ground state by radiationless decay [11].

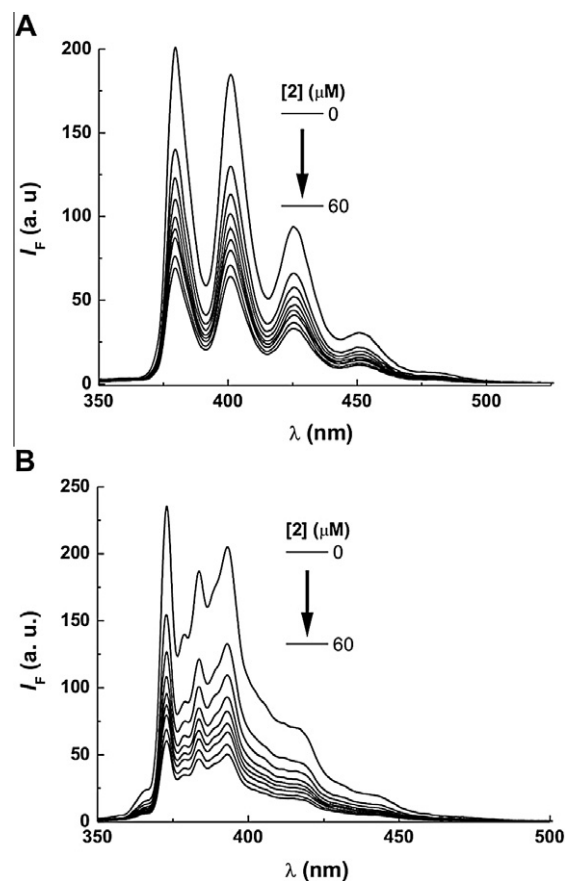


Fig. 3. Luminescence quenching of anthracene (A) ($\lambda_{\text{ex}} = 340$ nm) and pyrene (B) ($\lambda_{\text{ex}} = 336$ nm) with $[\text{Re}(\text{CO})_3(\mu\text{-OC}_5\text{H}_{11})]_4(\mu\text{-PCA})_2$, **2**, in THF at 25 °C.

Luminescent intensities versus quencher concentrations in all cases provided linear Stern–Volmer plots, suggesting dynamic or static quenching. In order to discern between both mechanisms, measurements were carried out at two temperatures (25 °C and 35 °C). Fig. 4 shows the Stern–Volmer plots for the quenching of the luminescence of anthracene by **2** at both temperatures in THF. The decrease in slope caused by a temperature increase is a clear indication of a predominant static quenching mechanism

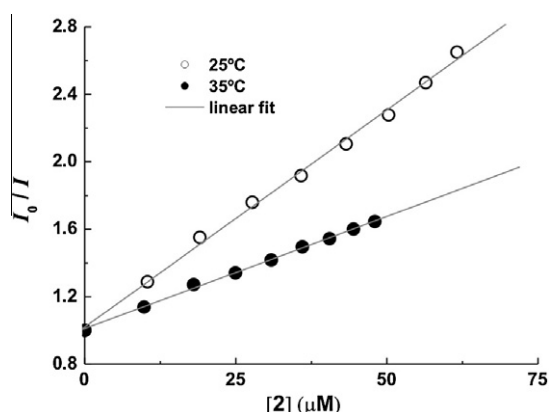


Fig. 4. Stern–Volmer plots for quenching of anthracene fluorescence with $[\text{Re}(\text{CO})_3(\mu\text{-OC}_5\text{H}_{11})_4(\mu\text{-PCA})_2]$, **2**, in THF at different temperatures ($\lambda_{\text{ex}} = 340$ nm, $\lambda_{\text{em}} = 401$ nm).

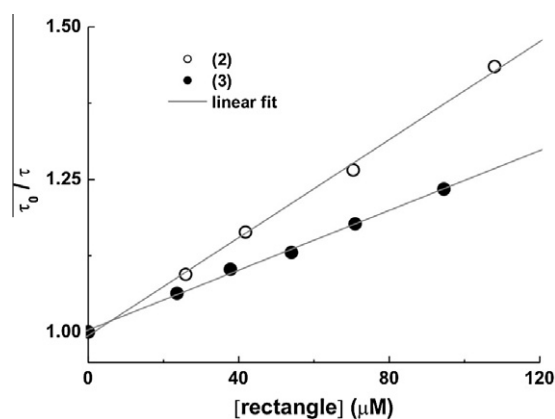


Fig. 5. Stern–Volmer plots of lifetime of excited pyrene vs. concentrations of **2** and **3** in THF at 25 °C ($\lambda_{\text{ex}} = 336$ nm, $\lambda_{\text{em}} = 373$ nm).

[13]. The same behavior (although to a lesser extent) was observed in the case of **3**.

Due to the short lifetime of excited anthracene, quenching experiments using lifetime measurements could only be done with pyrene in THF. Fig. 5 shows the Stern–Volmer plots obtained for both complexes at 25 °C.

In the analogous rectangular complexes with 4,4'-bpy as a bridging ligand [11], it has been proved that pyrene forms a charge-transfer complex with 4,4'-bpy stabilized by donor–acceptor interactions. The face of the guest pyrene is situated over the edges of the linkers.

All the Stern–Volmer constants are shown in Table 3. It can be concluded that quenching is more effective with pyrene than with anthracene and is less efficient in **2** than in **3**. On the other side, the

dynamic Stern–Volmer constants for pyrene were lower by almost one order of magnitude than the stationary Stern–Volmer constants for both complexes, indicating that the decay of fluorescence occurs predominantly under a static mechanism. Decreasing the size of the linkers that form the molecular rectangles from **2** to **3** induces a decrease in the association constant. These results are consistent with strong C–H··· π interactions, already reported in several systems, although it has been rarely designed into a host–guest pair [11,18,19]. The association constants shown in Table 3 are of the same order of magnitude of those reported before in similar systems [11], which leads to the conclusion that both guests are located over the edges of the linkers in **2** and **3**. Besides, it can also be envisaged that these compounds will present cytotoxicity against tumoral cells, based on molecular similarities [14].

Finally, it has recently been observed in molecular rectangles whose portal size is enough to accept entering small planar aromatic molecules that the association constant decreases when the aromatic surface of the guest molecule is diminished, a fact that can be explained on the basis of reduced π – π host–guest interactions [20]. By considering that the extent of C–H··· π interactions depend on the length of the linkers of the molecular rectangles, we conclude in this work that decreasing the length of a molecular rectangle by two C=N bonds (from PCA in **2** to 4,4'-azpy in **3**) reduces the interaction within the host–guest pair by a factor of 3.

5. Conclusions

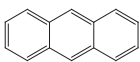

New alkoxy-bridged rhenium tricarbonyl complexes were synthesized and characterized by spectroscopic and diffraction techniques. They efficiently quench the luminescence of polycyclic aromatic hydrocarbons such as pyrene and anthracene. The quenching mechanism was predominantly static, indicating a strong interaction with these hydrocarbons. Although many rhenium-containing molecular rectangles show similar quenching mechanisms by small aromatic molecules [3], this is a novel study of the influence of the length of the cavity on host–guest C–H··· π interactions. The Stern–Volmer constants, of the order of 10^4 M⁻¹, were lower for **3** than for **2** in a factor of 3, indicating reduced interactions with decreasing length of the linkers of these molecular rectangles.

Acknowledgments

We would like to thank Universidad Nacional de Tucumán (UNT), Consejo Nacional de Investigaciones Científicas y Técnicas (CONICET), Agencia Nacional de Promoción Científica y Tecnológica (ANPCyT), all from Argentina, and MICINN (CTQ2010-21497) from Spain, for financial support. M.C. thanks CONICET for a graduate fellowship. F.E.M.V. also thanks CONICET for a postdoctoral fellowship. F.F. and N.E.K. are members of the Research Career from

Table 3

Values of Stern–Volmer constants obtained by intensity (stationary) and lifetime (dynamic) measurements.

	Stationary		Dynamic			
	$K_{\text{SV}} (\text{M}^{-1}) \times 10^{-3}$		$K_{\text{SV}} (\text{M}^{-1}) \times 10^{-3}$			
	(2)	(3)	(2)	(3)		
	25 °C	35 °C	25 °C	35 °C	25 °C	35 °C
Anthracene 	25.8 ± 0.6	12.8 ± 0.5	8.2 ± 0.3	7.3 ± 0.1	n.d.	n.d.
Pyrene 	30.0 ± 0.8	n.d.	10.9 ± 0.2	n.d.	4.1 ± 0.1	2.4 ± 0.1

CONICET, Argentina. We thank Eduardo Escudero-Adan for his help in the X-ray diffraction studies.

Appendix A. Supplementary material

Supplementary data associated with this article can be found, in the online version, at [doi:10.1016/j.ica.2011.02.075](https://doi.org/10.1016/j.ica.2011.02.075).

References

- [1] S. Sun, A.J. Lees, *Coord. Chem. Rev.* 230 (2002) 171.
- [2] C.-Y. Su, Y.-P. Cai, C.-L. Chen, M.D. Smith, W. Kaim, H.-C. zur Loye, *J. Am. Chem. Soc.* 125 (2003) 8595.
- [3] P. Thanasekaran, R.-T. Liao, Y.-H. Liu, T. Rajendran, S. Rajagopal, K.-L. Lu, *Coord. Chem. Rev.* 249 (2005) 1085.
- [4] Y.-F. Han, H. Li, G.-X. Jin, *Chem. Commun.* 46 (2010) 6879.
- [5] S. Sun, A.J. Lees, *Inorg. Chem.* 38 (1999) 4181.
- [6] R.V. Slone, D.I. Yoon, R.M. Calhoun, J.T. Hupp, *J. Am. Chem. Soc.* 117 (1995) 11813.
- [7] R.V. Slone, K.D. Benkstein, S. Bélanger, J.T. Hupp, I.A. Guzei, A.L. Rheingold, *Coord. Chem. Rev.* 171 (1998) 221.
- [8] S.M. Woessner, J.B. Helms, Y. Shen, B.P. Sullivan, *Inorg. Chem.* 37 (1998) 5406.
- [9] B. Manimaran, T. Rajendran, Y.-L. Lu, G.-H. Lee, S.-M. Peng, K.-L. Lu, *J. Chem. Soc., Dalton Trans.* (2001) 515.
- [10] P.H. Dinolfo, J.T. Hupp, *Chem. Mater.* 13 (2001) 3113.
- [11] B. Manimaran, L.-J. Lai, P. Thanasekaran, J.-Y. Wu, R.-T. Liao, T.-W. Seng, Y.-H. Liu, G.-H. Lee, S.-M. Peng, K.-L. Lu, *Inorg. Chem.* 45 (2006) 8070.
- [12] G.M. Sheldrick, *SHELXTL Crystallographic System Ver 6.14*, Bruker AXS Inc., Madison, Wisconsin, 2000.
- [13] J.R. Lakowicz, *Principles of Molecular Fluorescence*, second ed., Kluwer Academic, Plenum Publishers, New York, 1999.
- [14] D.K. Orsa, G.K. Haynes, S.K. Pramanik, M.O. Iwunze, G.E. Greco, J.A. Krause, D.H. Ho, A.L. Williams, D.A. Hill, S.K. Mandal, *Inorg. Chem. Commun.* 10 (2007) 821.
- [15] M. Cattaneo, F. Fagalde, N.E. Katz, *Inorg. Chem.* 45 (2006) 6884.
- [16] P.H. Dinolfo, M.E. Williams, C.L. Stern, J.T. Hupp, *J. Am. Chem. Soc.* 126 (2004) 12989.
- [17] G. Pourrioux, F. Fagalde, I. Romero, X. Fontrodona, T. Parella, N.E. Katz, *Inorg. Chem.* 49 (2010) 4084.
- [18] B.J. McNelis, L.C. Nathan, C.J. Clark, *J. Chem. Soc., Dalton Trans.* (1999) 1831.
- [19] J.M. Boncella, M.L. Cajigal, K.A. Abboud, *Organometallics* 15 (1996) 1905.
- [20] N.P.E. Barry, B. Therrien, *Eur. J. Inorg. Chem.* (2009) 4695.